(4)

OFFICE OF NAVAL RESEARCH

Contract N00014-80-K-0852

R&T Code_____

Technical Report No. 43

Review of Photoelectron and Auger Data for the High-Temperature SUperconductors

By

D. E. Ramaker

Prepared for Publication

in the

America Vacuum Society Series 3 (AIP Conf. Proc. 165.)

George Washington University
Department of Chemistry
Washington, D.C. 20052

December, 1988

ADA202079

SECURITY CLASSIFICATION OF THIS PAGE

REPORT DOCUMENTATION PAGE

1a. REPORT SECURITY CLASSIFICATION: Unclassified	1b. RESTRICTIVE MARKINGS
2a. SECURITY CLASSIFICATION AUTHORITY	3. DISTRIBUTION / AVAILABILITY OF REPORT: Approved for Public Release, distribution Unlimited.
2b. DECLASSIFICATION / DOWNGRADING SCHEDULE	
4. PERFORMING ORGANIZATION REPORT NUMBER(S): Technical Report # 43	5. MONITORING ORGANIZATION REPORT NUMBER(S)
6a. NAME OF PERFORMING ORGANIZATION: Dept. of Chemistry, George Washington Univ. / 6b. OFFICE SYMBOL (If applicable)	7a. NAME OF MONITORING ORGANIZATION: Office of Naval Research (Code 413)
6c. ADDRESS (City, State, and ZIP Code): Washington, D.C. 20052	7b. ADDRESS (City, State, and ZIP Code): Chemistry Program, 800 N. Quincy Street, Arlington, VA 22217
8a. NAME OF FUNDING / SPONSORING ORGANIZATION: Office of Naval Research / 8b. OFFICE SYMBOL (If applicable)	9. PROCUREMENT INSTRUMENT IDENTIFICATION NUMBER: Contract N00014-80-K-0852
8c. ADDRESS (City, State, and ZIP Code): Chemistry Program, 800 North QUINCY, Arlington, VA 22217	10. SOURCE OF FUNDING NUMBERS: PROGRAM ELEMENT NO. 61153 N; PROJECT NO.; TASK NO. PP 013-08-01; WORK UNIT ACCESSION NO NR 056-661

11. TITLE (Include Security Classification): Review of Photoelectron and Auger Data for the High-Temperature Superconductors (Uncl.)

12. PERSONAL AUTHOR(S): D. E. Ramaker

13a. TYPE OF REPORT	13b. TIME COVERED	14. DATE OF REPORT (Year, Month, Day)	15. PAGE COUNT
Interim Technical	FROM _____ TO _____	December 1988	10

16. SUPPLEMENTARY NOTATION: Prepared for publication in America Vacuum Society Series 3(AIP Conf. Proc. 165.)

17. COSATI CODES		
FIELD	GROUP	SUB-GROUP

18. SUBJECT TERMS (Continue on reverse if necessary and identify by block number): Superconductivity, Photoelectron Spectroscopy, Auger Spectroscopy, Electron Correlation, Copper oxides, Theory

19. ABSTRACT (Continue on reverse if necessary and identify by block number)

A review of the photoelectron and Auger data reported for the recently discovered high temperature superconductors reveals that the surfaces of these materials are highly reactive to adsorbed gases. The Cu-O bonds appear to be highly covalent, indeed, the Cu-O covalency increases with Tc in these materials. The screening response to creation of a core hole, as reflected in the LV-VVV Auger satellite, is suggestive of the excitonic mechanism for the superconductivity.

20. DISTRIBUTION / AVAILABILITY OF ABSTRACT	21. ABSTRACT SECURITY CLASSIFICATION
☒ UNCLASSIFIED/UNLIMITED ☒ SAME AS RPT ☐ OTIC USERS	Unclassified
22a. NAME OF RESPONSIBLE INDIVIDUAL: Dr. David L. Nelson	22b. TELEPHONE (Include Area Code): (202) 696-4410 / 22c. OFFICE SYMBOL

DD FORM 1473, 84 MAR — 83 APR edition may be used until exhausted. All other editions are obsolete.

SECURITY CLASSIFICATION OF THIS PAGE: Unclassified

88 12 13 070

REVIEW OF PHOTOELECTRON AND AUGER DATA FOR THE HIGH TEMPERATURE SUPERCONDUCTORS

D.E. Ramaker
Naval Research Laboratory, Washington, DC 20375

ABSTRACT

A review of the photoelectron and Auger data reported for the recently discovered high temperature superconductors reveals that the surfaces of these materials are highly reactive to adsorbed gases. The Cu-O bonds appear to be highly covalent, indeed, the Cu-O covalency increases with T_c in these materials. The screening response to creation of a core hole, as reflected in the LV-VVV Auger satellite, is suggestive of the excitonic mechanism for the superconductivity.

INTRODUCTION

The recent discoveries[1,2] of superconductivity above 30 K in $La_{2-x}Ba_xCuO_4$ and above 90 K in $YBa_2Cu_3O_{7-x}$ have resulted in a number of recent papers reporting spectroscopic investigations on these superconducting (SC) materials (herein called the doped La and 123 materials). This work examines and reviews those papers reporting core level XPS (X-ray photoelectron spectroscopy) and Cu AES (Auger electron spectroscopy) data. Those papers reporting valence band photoemission data and core level absorption spectra are reviewed by Kurtz[3] and Onellion[4] in separate papers to appear in these proceedings. All papers, published and in the preprint stage, of which the author is aware, are reviewed. Considering the rate at which these papers are appearing, it is inevitable that some may have been overlooked; the author apologizes for those missed.

This work is of necessity preliminary in nature. The spectroscopic data have been found to be very dependent on the sample preparation procedures, surface treatment, and exposure. Conflicting interpretations of even the same data have also been reported. Much additional spectroscopic work needs to be done. An attempt is made to point out where additional data would be particularly helpful.

A brief summary of the properties and preparation procedures for the two types of superconductors will be helpful for later discussions. The superconducting phase of the doped La material has been identified as having the tetragonal K_2NiF_4 structure. A small orthorhombic distortion from the K_2NiF_4 structure occurs at 533 K in La_2CuO_4. Doping with Sr or Ba stabilizes the tetragonal structure at lower temperatures; however, the structural transition temperature, T_d, still apparently falls above the superconducting transition temperature, T_c, for almost all Sr doped levels[5]. The rate of cooling from the O anneal is apparently critical to the quality of the superconducting sample[5,6]. The 123 material also exists in two different crystal structures. In this case, the tetragonal material

(123-t) has a composition with x around 0.5 and a disordered array of O vacancies. The resulting structure has two-dimensional arrays of Cu-O bonds and a T_c similar to that for doped La[7]. It can be prepared by fast cooling after the O anneal. Slow cooling increases the total O present (i.e. reducing x), allows the remaining O vacancies to order, and produces the orthorhombic structure (123-o). This ordering introduces one dimensional chains of CuO_4 bonds which is believed to be instrumental in producing the higher T_c[7].

This paper is divided into sections which review the O K, the Sr, Y, La, and Ba M_{45}, and the Cu L_{23} XPS data, and the Cu $L_{23}VV$ AES data. A section interpreting a possible temperature dependence of the data is also included, followed by a summary.

THE O K LEVEL

Fig. 1 shows O 1s XPS data for the two SC materials, and its observed dependence on sample preparation, surface exposure time, electron take-off angle, and sample temperature. The data reported by Schrott et al.[8] arise from 123 samples prepared by annealing in

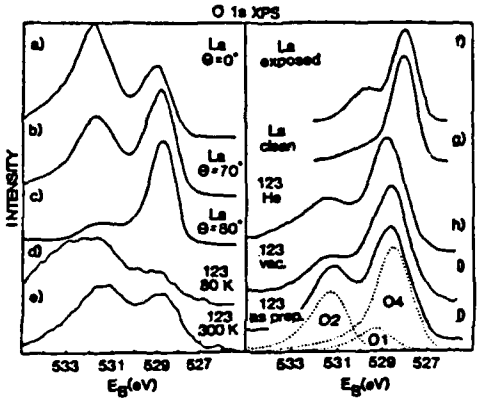

Fig 1. Comparison of O 1s XPS data for the superconducting 123 and doped La materials.

a-c) Al Kα spectra from $La_{1.85}Ba_{0.15}CuO_4$ for electron escape angles Θ measured with respect to the surface normal. From Ref. 14.

d-e) Mg Kα spectra from $YBa_2Cu_3O_{7-y}$ measured at 300 and 80 K. From Ref. 15.

f-g) Al Kα spectra from a $La_{1.85}Sr_{0.15}CuO_4$ clean cleaved and exposed surface (5×10^{-11} Torr for 14 hrs). From Ref. 11.

h-j) Mg Kα spectra from $YBa_2Cu_3O_{7-z}$ annealed in flowing He at 500°C (T_c = 33 K), heated in vacuum at 450°C (T_c = 84 K), and as prepared (T_c = 91 K). From Ref. 8.

O, subsequently annealed in vacuum at 450 °C, or heat treated in flowing He, respectively. They resolved the spectra into 3 contributions as shown, and assigned the contributions to O atoms in the two-dimensional Cu-O planes (O4), to those in the Cu-O chains (O1), and those in the Ba-O planes (O2). From this analysis, they assert that removal of O2 only slightly decreases the T_c from 90 K, while removal of O1 atoms dramatically reduces T_c to 50 K. They conclude that the one-dimensional Cu-O chains are important to the high T_c superconductivity.

The exact nature of the 531.5 eV feature in the O XPS data is rather controversial, however. Schrott et al.[9] acknowledge that the feature at 531.5 eV was sensitive to adsorbed water; however, they scraped the sample repeatedly under vacuum, removing up to several hundred microns of material, until no further change in the photoemission spectra was observed. They concluded that the 531.5 ev feature is indeed representative of O2 sites in the bulk. Yarmoff et al.[9] see features at 531 and 528 eV with an intensity ratio of 4.2:1. They assign the 531 eV feature to both the O2 and O4 sites, and the 528 eV feature to the O1 sites. Ihara et al.[10] talk of vertical and horizontal sites in the octahedron of the Sr doped La material, the vertical sites in the La,Sr-O plane having higher binding energy than the horizontal sites in the Cu-O planes.

On the other hand, Hill et al.[11] saw only a long tail extending up to 532 eV in the XPS from a clean cleaved surface of the Sr doped La material. Only after exposures of up to 14 hrs at $5x10^{-11}$ Torr pressures did they see a feature at around 530 eV (see Fig. 1). Nucker et al.[12] on a similar material was able to remove essentially all of the 531-533 eV feature by scraping a few tenths of a millimeter of material from the surface. They concluded that this feature (originally 30%) was due to adsorbed impurities such as hydroxides. Iqbal et al.[13] on the 123 material found that scraping decreased the high energy peak, while in-situ exposure to air increased it. Steiner et al.[14] on 123 also obtained a 30% feature at 531 eV (see Fig. 1), but observed that it increased by a factor of ten when going from normal emission to a glancing take-off angle of 80° with respect to the sample normal (see Fig. 1). They concluded that this feature was mostly due to adsorbed CO, CO_2 and OH. Sarma et al.[15] for the 123 material reported two equal peaks (see Fig. 1), and assigned the 531.5 eV peak to adsorbed hydroxyl ion. The only authors to report a spectrum at 80 K, they find an additional peak at 533.3 eV (see Fig. 1), which they attributed to O_2^{2-} ions resulting from O dimerization below T_c.

What are we to conclude from all of this? The absence of the 531 eV feature on clean cleaved surfaces, the ability to nearly remove the 531 eV feature by heavy scraping, and its observed take-off angle dependence, indicate strongly that at least a major portion of it arises from adsorbed impurities. If one accepts this, then the expected atomic ratios (i.e. there should be 4-O4, 1-O2 and 1-O1 sites per unit cell in the 123 material) are not reflected in the XPS spectra, regardless of whether the 531 eV feature is assigned to the O2 or O2 + O4 sites. Below T_c, the sample probably acts as a "cryogenic pump" so that the additional peak at 533.3 eV observed

by Sarma et al.[18] probably results from water in the second and higher layers on the surface (the O 1s binding energy in bulk water is around 534 eV). Thus it seems safe to conclude that the entire 532-534 eV feature arises from adsorbed species, and that the O sites all have similar binding energies. This is an important result which would not be expected in a highly ionic system. It suggests that all of the O atoms are involved in relatively strong covalent bonds with the Cu atoms.

THE Sr, Y, Ba, AND La M_{45} CORE LEVELS

The Sr, Y, Ba, and La M_{23} or 3d core levels behave similarly. The results can be briefly described as follows:

The Sr 3d XPS data for SrO reveal two peaks split by about 1.6 eV as a result of spin orbit splitting[16]. In doped La materials, a second doublet about 1.4 eV higher in energy appears. The relative intensities of these two doublets vary with sample preparation; the second component being particularly large for a partially superconducting Sr doped La material[16].

The Y 3d XPS data for Y_2O_3 reveal two peaks split by about 1.9 eV as a result of spin orbit splitting[13]. In the 123 material a second doublet about 1.4 eV higher in energy appears. In a series of samples (i.e. preannealed, O annealed, scraped, exposed to air in-situ, etc.) the second doublet appears to increase in intensity as the O 1s higher binding energy feature increases in intensity[13].

The Ba $3d_{5/2}$ XPS data for BaO_2 reveals a single peak at 779 eV[13]. For a series of 123 samples (as above), peaks appear at around 780 and 778 eV, the intensity of the 780 eV feature tracking with the intensity of the higher binding O 1s peak[13]. Data taken at several take-off angles for a Ba doped La sample revealed peaks at 779 and 780.5, the 780.5 eV peak growing with larger angle with respect to the normal; i.e. the 780.5 eV peak reflects species more on the surface[14].

The La $3d_{5/2}$ XPS data for ionic La^{3+} compounds reveal two peaks separated by about 5.3 eV[14]. These spectra have been studied extensively both theoretically and experimentally[17]. The two peaks are attributed to $4f^0$ and $4f^1\underline{L}$ final state configurations in the presence of the 3d core hole. The latter configuration indicates a charge transfer process from the ligand into the La 4f orbital to screen the core hole. In the La materials these two peaks change their relative intensities with take-off angle, the lower peak decreasing at larger take-off angles; i.e. the screened contribution decreases in intensity for species near the surface[14].

Steiner et al.[14,16] propose that the higher binding energy features arise because of the presence of O defects near the metal ions. It is suggested that the defects are less polarizable than O atoms, causing the core binding energy of the neighboring metal ions to be larger. But the data would then indicate that the concentration of defects is larger near the surface, and that it is larger when O impurities (i.e. OH or CO_x) are on the surface. More likely, the higher binding energy features arise because of the presence of OH and CO_x species, i.e. the formation of metal

hydroxides or carbonates[11,12]. These species are expected to be less polarizable and more ionic than O atoms twice bonded in the lattice. It has been previously indicated that the interaction of H_2O with both the La and the 123 SCs decreases the superconducting volume fraction and forms hydroxide and carbonate species[10].

THE CU L_{23} LEVELS

The Cu L_{23} levels, compared to all the other core levels, have been the most discussed in the literature. Fig. 2 compares the Cu L_{23} XPS data for Cu metal (Cu^0), Cu_2O (Cu^{1+}), and CuO (Cu^{2+}) where the nominal Cu valence states are indicated in parentheses[19]. Some trends are clear. The L_3 binding energy increases as the Cu valence state increases. Only Cu^{2+} exhibits a large satellite around 942 eV, and a very large width for the principal L_3 peak. Comparison of these spectra with those for undoped La (Cu^{2+}) and 123-o (2/3 Cu^{2+} and 1/3 Cu^{3+}) suggests at the outset that the Cu is primarily in the Cu^{2+} state in these materials.

The very large widths of the L_{23} peaks for the doped La and 123-o materials have been interpreted a number of different ways. Ihara et al.[10] divided the L_3 experimental peak into 3 contributions located at 931.5, 932.6, and 934.2 eV, each with a gaussian width of 1.56 eV. These three peaks were attributed to Cu atoms in the +1, +2, and +3 valence states, respectively, with an intensity ratio of 1:2:1. Hill et al.[11] suggested that the L_3 peak has contributions from

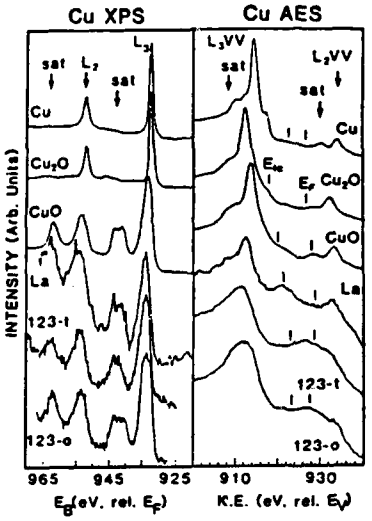

Fig. 2 Comparison of Cu L_{23} XPS and $L_{23}VV$ AES data for Cu, Cu_2O, CuO, La_2CuO_4, and for $YBa_2Cu_3O_{7-x}$ in the "tetragonal" and orthorhombic crystal structures (i.e., the La, 123-t and 123-o materials). These data are summarized in Table I along with the reported T_c. The principal components, L_2 and L_3, and satellites for each case are indicated. The vertical marks indicate the energy of the L_3 Fermi level, E_f, and the two-center feature, E_{ac}. From Ref. 19.

both Cu^{1+} and Cu^{2+}. Alvarado et al.[20] fit two Doniach-Sunjic lineshapes separated by 2 eV to the L_3 peak and determined that both of the SC materials have around 40% Cu^{2+} and 60% Cu^{2+}. These approaches seem unlikely however, because the L_3 peak for CuO is equally wide, and only Cu^{2+} is present in CuO. Indeed, Steiner et al.[21] attempted to synthesize the 123-o L_3 spectrum by a combination of the CuO and $NaCuO_2$ (Cu nominally in the Cu^{3+} state) spectra, and concluded that the 123-o spectrum reflected primarily Cu^{2+}.

A theoretical explanation for the large width of the L_3 XPS peak in CuO and the superconductors has been given by van der Laan et al.[22]. They observed in the copper halides that the L_3 width decreased as the satellite peak intensity decreased. In the series CuF_2, $CuCl_2$, and $CuBr_2$, the width (roughly at 5.0, 3.6, and 3.0 eV) decreased as the relative satellite intensity, I_s/I_m, decreased (0.8, 0.6, and 0.45)[22]. Thus the CuO and the SC L_{23} XPS peaks are broad apparently because large satellite contributions are present.

The main and satellite peaks, according to the theory of Larsson[23], correspond mainly to $2p^53d^{10}$ and $2p^53d^9$ final states, respectively; i.e. to Cu^{1+} and Cu^{2+}. These are nominal electronic configurations which ignore hybridization with the ligand valence electrons. Van der Laan et al.[22] refer to these states as $\underline{2p}3d^{10}\underline{L}$ and $\underline{2p}3d^9$, where $\underline{2p}$ and $\underline{L}$ indicate holes are present in the Cu 2p core level and on the neighboring ligand. The main peak corresponds to a more fully screened final state, and the satellite can be thought of as arising from a bonding to antibonding, σ to σ^*, shakeup transition, which in an ionic picture is effectively a charge transfer from the Cu to the ligand[23]. The satellite is broad, and even shows structure, because of multiplet splitting in the $\underline{2p}3d^9$ final state[22]. Such multiplet splitting is absent in the $\underline{2p}3d^{10}\underline{L}$ final state because the 3d shell is now filled.

The satellite intensity and main peak broadening arise because the true eigenstates for the ground and XPS final states are linear combinations of the $3d^9$ and $3d^{10}\underline{L}$ configurations, without and with a 2p core hole[22]. The satellite intensity in the sudden approximation depends on the change in mixing as a result of the 2p hole, and the width of the L_3 XPS peak depends on the amount of $\underline{2p}3d^9$ mixed into the eigenstate for the principal final state.

In summary, the satellite intensity and main peak width are correlated, as seen in experimental spectra and explained by the theory. To reiterate, the Cu XPS spectra for the doped La and 123-O materials reflect primarily Cu^{2+}. In fact, Fujimori et al.[24], using the model of Larsson and van der Laan to interpret the Cu XPS data, indicate that in the ground state, the 3d electron occupancy is 9.45, or the average valence of Cu is 1.55 in both the Sr doped La and 123-o SCs. Thus in this model the average Cu valency is not even +2. This is consistent with the covalent character of the Cu-O bonds as indicated by the XPS data, to be discussed below, and the presence of 2p features in O K level x-ray absorption spectra[9].

Although the Cu XPS for the SCs are rather similar, Fig. 2 and Table I show[19] that the relative satellite intensity, I_s/I_m, decreases, and the energy separation, ΔE_{ms}, slightly increases, systematically down the series CuO, undoped La, 123-t, and 123-o. The 123-t

TABLE I Summary of the XPS and AES data for the five materials studied by Ramaker et al.[19].

Item	Cu_2O	CuO	La	123-t	123-o
T_c(K)	-	-	43-29	80-70	93-91
XPS					
ΔE_{ss}[a] (eV)	-	8.7	8.5	9	9.2
I_s/I_m[a,b]	-	0.58	0.49	0.43	0.37
AES					
$I(L_3V\text{-}VVV)/I(L_3VV)$[a], Exp.	0.75	0.75	1.3	1.3	1.4
% of shakeup transferred to $L_3V\text{-}VVV$	0	0	77	85	100
$[E_p\text{-}E_f]$[a] (eV)	15.7	16.0	16.3	16.5	15.0
$[E_{cc}\text{-}E_f]$[a] (eV)	8.9	8.2	7.7	5.6	4.4

[a]Estimated uncertainties in these data are indicated in Ref. 19.
[b]Iqbal et al.[13] find I_s/I_m is 0.44 for CuO and 0.34 for the 123 material.

material was air quenched from 900°C instead of slow cooled, so that it contains some fraction of the tetragonal phase. The undoped La material exhibited only a resistivity minimum around 29 K, however recent reports suggests that it may exhibit a filamentary superconductivity below 40 K under certain conditions[25]. Table I gives the temperature for each SC material at which the resistance begins to drop with cooling, and the temperature at which the resistance drops to zero. Table I reveals a reverse correlation of satellite intensity, I_s/I_m, with T_c among the various materials.

This reverse correlation has been found by other investigators[13]. The data of Steiner et al[16] shown in Fig. 3 reveals that as x increases from 0 to 0.2 in $La_{2-x}Sr_xCuO_4$, the Cu^{2+} satellite decreases and T_c increases. Indeed, they find that in a fast cooled sample with x = 0.2, but which is only partially superconducting, the Cu^{2+} satellite is again increased. Within the Larsson-van der Laan model, a decreasing I_s/I_m and increasing ΔE_{ss} indicates a decreasing electronegativity of the ligands[22]. We conclude that the Cu-O covalency of the SCs increases as T_c increases, or from another perspective, the number of O holes increases as T_c increases. This correlation between number of O holes and T_c has been observed before[26].

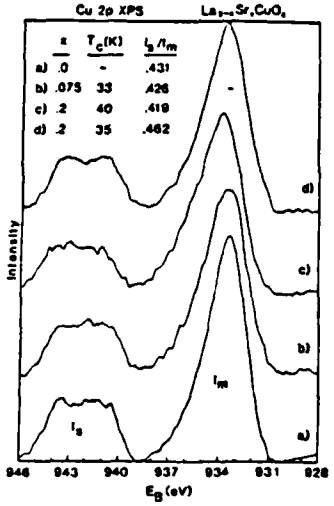

Fig. 3 Cu L_{23} XPS spectra for various $La_{2-x}Sr_xCuO_4$ samples from Ref. 16. The spectra are normalized to have the same total area. An identical linear background has been subtracted from each spectrum. x, T_c, and I_s/I_m are given for each case. Sample d was only partially superconducting.

One apparent exception to the above correlation occurs when the doping level is increased substantially above 0.2. Fujimori et al.[24] find for $x = 0.5$ and Ihara et al.[16] for $x = 0.6$ that the materials may be non-superconducting or have a lower transition temperature, but the satellites are still decreased. However, Shafer et al[25] indicate that for x greater than 0.2, the number of O vacancies increases substantially, and therefore the number of O holes decreases. The decreased satellite in this case does not arise from decreased covalency within the CuO_4 planes, but from the presence of increased amounts of Cu^{1+} in the CuO_{4-y} planes[16].

Unlike the O 1s and metal 3d XPS spectra discussed above, the Cu 2p spectra do not exhibit a high sensitivity to surface preparation and exposure; indeed, Steiner et al.[21] find that the Cu spectrum does not change with take off angle. However, in a series of surface treatments as described above, Iqbal et al.[13] find that the I_s/I_m ratio changes. This ratio is the largest after annealing in O_2 or exposure to air, and is smallest after scraping the surface. This suggests that CuO, which exhibits the largest I_s/I_m ratio, is formed on the surface, along with the metal hydroxides and carbonates, upon exposure of the surface to air, H_2O, or even O_2.

THE Cu $L_{23}VV$ AUGER SPECTRA

Fig. 2 compares the Cu $L_{23}VV$ Auger lineshapes[19] for Cu metal, Cu_2O, CuO, and the undoped La, 123-t, and 123-o SCs (the latter 3 materials have been described above). The L_3VV lineshapes reveal a principal peak around 915 eV, and a satellite around 908 eV. The

principal peak is known to arise from the normal L_3VV process, the satellite from the L_3V-VVV process. A clear trend in the relative satellite intensities exists. I(LV-VVV)/I(LVV) is relatively constant for Cu, Cu_2O and CuO. For the "SCs", I(LV-VVV)/I(LVV) is much larger, and it increases while I_s/I_a in the XPS decreases (see Table I). This trend is also seen in the data of Iqbal et al[13] for the different 123-o surface treatments as described above. It is also apparent in the data of Fuggle et al.[27], although less clear.

An explanation for this trend has been given by Ramaker et al.[19]. They attribute the Auger satellite in Cu, Cu_2O, and CuO to a combination of the Coster-Kronig and shakeoff processes. The L_1 and L_2 core holes may undergo Coster-Kronig decay ($L_{12}L_3V$). The resultant L_3 core hole may subsequently Auger decay, and because of the extra valence hole, this results in the satellite. The shakeoff process involves loss of a valence electron as a result of sudden creation of a core hole, i.e. it is a relaxation effect. The additional valence hole in the initial state, provides a 3-hole final state after the Auger process. These two processes can cause satellite intensities up to 70% of the principal peak intensity in close agreement with experiment for the non-SCs[19].

The additional Auger satellite intensity for the SCs was attributed to the σ to σ^2 shakeup process which produces the XPS satellite[19]. Normally, shakeup does not cause a satellite Auger contribution since both the shakeup electron and hole remain localized, and consequently the shakeup-Auger final state effectively contains only two holes (i.e., the 3-hole, 1-electron final state has a similar net repulsion energy as a 2-hole state). However, if the σ^2 electron should propagate away before the core hole decay, a local 3-hole final state results. The σ^2 electron does not propagate away in CuO because the s^2 orbital on the atom with the core and valence holes drops out of the conduction band and becomes a localized excitonic-like state. In the SCs, no band gap exists, so that the σ^2 electron propagates away with increasing probability as the covalency of the Cu-O bond increases. Since I_s/I_a decreases as I(LV-VVV)/I(LVV) increases, apparently the σ^2 shakeup electron does not always escape before the Auger decay. The probability for escape in each case can be determined empirically from the experimental Auger satellite intensity; this is given in Table I[19].

The features seen in Fig 2 between the L_3 and L_2 Auger contributions (indicated by the vertical hatch marks) have been attributed to an effective two-center Auger final state[19,22]. Such a final state might arise when the σ Cu-O bonding band is involved in the Auger decay, in contrast to the non-bonding or weakly π Cu-O bonding bands which dominate the principal feature. Fig. 2 and Table I show that the energy of this two-center feature relative to the Fermi level (i.e. E_{tc}-E_f) decreases with increasing covalency. The two-center U_{eff} decreases as the covalency increases, because of the increased screening of the Cu-O valence holes by the more delocalized σ electrons in the more covalent systems. However, the σ electrons are apparently ineffective at screening the more localized holes in the π orbitals, since E_p-E_f is relatively constant, except in 123-o. Recent band structure calculations[28] indicate that a π^2 band

in 123-o may not be completely filled, so that in this case some of the π electrons can effectively screen the Auger π holes.

THE TEMPERATURE DEPENDENCE OF THE XPS AND AES DATA

A limited amount of XPS and AES data has been reported for samples at low temperatures. Sarma et al[15] reported the Cu L_{23} XPS and $L_{23}VV$ AES data for 123-o at 80 K shown in Fig. 4. They see a reduced XPS satellite and an enlarged Auger satellite, i.e. a continuation of the trend discussed above. Iqbal et al.[13] report data for 123-o samples at 170 K and see a similar trend. In addition they see a reduction in the valence band Cu satellite with E_B around 10-16 eV. In contrast, Thiry et al.[29] see a larger valence band satellite for 123-o samples at 81 K. The valence-band Cu satellite has an origin not unlike the core level Cu satellite. In all three instances, these trends were perfectly reproducible and reversible as the materials were cycled from ambient to lower temperatures. Only after repeated cycles do these trends tend to diminish, apparently due to deterioration of the surface layers, which are reflected in the spectra.

The effects of impurities such as H_2O on the surface must be of great concern at these low temperatures. As discussed above, samples at these temperatures act as "cryogenic pumps" for H_2O producing bulk-like H_2O features in the O 1s XPS data of Sarma et al.[15]. However, the data of Iqbal et al.[13] show that exposure to air or O_2 causes the satellite trends to go in the opposite direction, i.e. an increased XPS satellite and a decreased Auger satellite. Therefore the core level trends noted above may reflect a property of the bulk

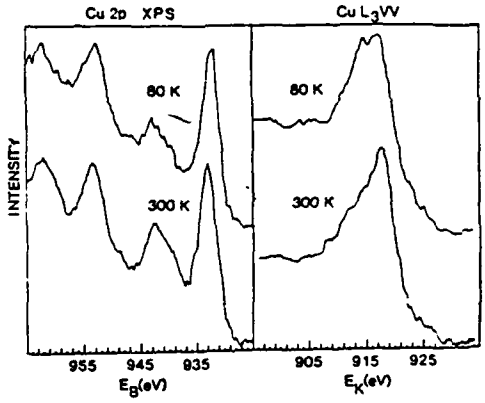

Fig. 4 Comparison of Cu L_{23} XPS data and L_3VV data for $YBa_2Cu_3O_{7-\epsilon}$ at 300 K and 80 K from Ref. 15.

at lower temperatures. The situation in the valence band region is much less clear. In the valence band region, the presence of H_2O or other impurities on the surface can increase the XPS signal, and beam damage can decrease the signal, just where the Cu satellite falls[3].

A solid has three ways of responding to creation of a core hole. These include atomic relaxation, charge transfer, and polarization. Each of these responses introduce primarily different dynamic or virtual excitations. Atomic relaxation enters through shakeoff, charge transfer through shakeup, and polarization through electron-hole (e-h) pair excitations[20]. Shakeoff is primarily responsible for the long featureless tail to lower energies in a core level XPS spectrum, shakeup is responsible for the satellite feature such as that already discussed, and e-h pair excitations are responsible for the slight tailing off of the primary peak giving it the Doniach-Sunjic lineshape often seen in metals. Similar e-h pair excitations also introduce the well-known edge singularity in XES and XAS data.

In light of the above, a significant reduction in the XPS satellite below T_c is not unexpected. At lower temperatures, particularly below T_c, one might expect polarization effects to increase, and thus charge transfer effects to decrease. However, if I_s/I_m is significantly decreased, then the width of the primary peak should decrease. The fact that the experimental data in Fig. 4 don't show this may be evidence that the effects of e-h pair excitations are indeed increased below T_c. Fig. 3 shows that the tailing off of the L_3 peak is the most pronounced for sample (c), i.e., the one with the highest T_c when the satellite is the smallest. This strongly suggests that e-h pair excitations are also occurring at room temperature; an expected result since these materials are metallic at room temperature. Edge singularity effects may also be present in recently reported O K XES and transmission EELS data, spectra which are more representative of the bulk. A feature occurring right at the Fermi level in the O K EELS data is seen to grow with increasing Sr doping level in the La SC material[12]. O K XES data for the 123 material shows a slight enhancement near the Fermi level[21].

The effects of e-h pair excitations on the L_3VV Auger lineshape for the SC's are quite different from that for normal metals, where only small effects are seen. In the 123-o material, all of the shakeup probability has already been utilized to account for the Auger satellite found at ambient temperatures. If indeed the Auger satellite increases and the XPS satellite decreases at lower temperatures, the increasing Auger satellite must result from the increasing e-h pair excitations. For this to be true, it means that the e-h excitation must effectively be a charge transfer from the Cu to the O or least from a localized state on the Cu atom to a more itinerant state. This is necessary so that the Cu ends up with a three-hole final state after the Auger decay to produce the LV-VVV satellite. It is also exactly what one would expect from the band calculations which indicate an occupied d_{xy} (π) like band just below the Fermi level, and a more itinerant $d_{x^2-y^2}$ (σ^*) like band just above it[28]. The Cu

to O or localized to itinerant electron transfer is similar to that suggested by the several different excitonic models for superconductivity, which is believed to be responsible for the electron pairing[21-25]. These charge transfer e-h pair excitations probably also contribute some intensity to the LV-VVV satellites for the SC materials at room temperature.

The above should not be taken as direct evidence for the excitonic models of superconductivity. Much more experimental data must be taken to sort out the effects of adsorbed surface species and/or beam damage and true low-temperature bulk effects. Furthermore, e-h pair excitations are a normal screening response and their localized to itinerant nature is consistent with the bulk-band structure calculations. Therefore, even if these excitations do occur, although suggestive, they do not necessarily establish the nature of the superconductivity.

SUMMARY

Review and interpretation of the XPS and AES data indicates the following:

1. The surface of the SCs is highly reactive to adsorbed gases, producing metal hydroxides or carbonates, and perhaps CuO near the surface, and significantly affects the XPS data.
3. The σ and σ^* Cu-O bonds appear to be highly covalent in the SCs, indeed the Cu-O covalency increases with T_c. This high covalency indicates that the holes are shared by both the Cu and O atoms, and the average Cu valency is estimated to be less than 2+.
3. The three dynamic effects of the screening response, namely shakeoff, shakeup, and e-h pair excitations, all contribute to the LV-VVV Auger satellite. The charge transfer nature of the e-h pair excitations is suggestive of the excitonic mechanisms for the superconductivity.

REFERENCES

1. J.G. Bednorz and K.A. Muller, Z. Phys. B64, 189 (1986).
2. M.K. Wu et al., Phys. Rev. Lett. 58, 908 (1987).
3. R. Kurtz, these proceedings.
4. M. Onellion, these proceedings.
5. R.M. Fleming, B. Batlogg, R.J. Cava, and E.A. Rietman, Phys. Rev. B35, 5337 (1987); Phys. Rev. Lett. 58, 408 (1987).
6. C. Politis, J. Geerk, M. Dietrich, and B. Obst, Z. Phys. B66, 141 (1987).
7. R.J. Cava et al., Phys. Rev. Lett. 58, 1676 (1987); J.E. Greedan et al., Phys. Rev. B35, 8770 (1987); A.J. Panson et al., Phys. Rev. B35, 8774 (1987); F. Beech et al., Phys. Rev. 35, 8778 (1987).
8. A.G. Schrott, S.I. Park, and C.C. Tsuei, preprint.
9. J.A. Yarmoff et al., Phys. Rev. B36, 3967 (1987).
10. H. Ihara et al., Japan J. Appl. Phys. 26, L460 (1987); L463 (1987).

11. D.M. Hill et al., Phys. Rev. B36, 3971 (1987).
12. N. Nucker et al., Z. Phys. B67, 9 (1987).
13. Z. Iqbal et al., J. Mat. Res., preprint.
14. P. Steiner et al., Appl. Phys. A44, 75 (1987).
15. D.D. Sarma, K. Sreedhar, P. Ganguly, and C.N.R. Rao, Phys. Rev. B36, 2371 (1987).
16. P. Steiner et al., Z. Phys. B66, 275 (1987); 67, 19 (1987).
17. A. Kotani et al., J. Phys. Soc. Japan 56, 798 (1987); Phys. Scripta, 35, 566 (1987).
18. K. Kishio et al., Japan J. Appl. Phys. 26, L466 (1987); M.F. Yan et al., Appl. Phys. Lett. 51, 532 (1987).
19. D.E. Ramaker et al., Phys. Rev. B36, xxx (1987).
20. F.G. Alvarado et al., Sol. State Commun. 63, 507 (1987).
21. P. Steiner et al., Z. Phys. B67, 497 (1987).
22. G. van der Laan, C. Westra, C. Haas, and G.A. Sawatzky, Phys. Rev. B23, 4369 (1981).
23. S. Larsson, Chem. Phys. Lett. 40, 362 (1976).
24. A. Fujimori, E.T. Muromachi, Y. Uchida, and B. Okai, Phys. Rev. B35, 8814 (1987).
25. P.M. Grant et al., Phys. Rev. Lett. 58, 2482 (1987).
26. M.W. Shafer, T. Penney, and B.L. Olson, Phys. Rev. B36, 4047 (1987); D.M. Newns, preprint.
27. J.C. Fuggle et al., Phys. Rev., preprint.
28. J. Yu, S. Massidda, A.J. Freeman, and D.D. Koelling, Phys. Lett. A122, 203 (1987); 198 (1987).
29. P. Thiry et al., preprint.
30. D.E. Ramaker, Phys. Rev. B25, 7341 (1982).
31. K.L. Tsang et al., preprint.
32. C.M. Varma, S. Schmitt-Rink, E. Abrahams, Sol. State Commun. 62, 681 (1987); and preprint.
33. W.A. Little, Phys. Rev. 134, A1416 (1964); and preprint.
34. J. Ihm and D.H. Lee, Sol. State Commun. 62, 825 (1987); and preprint.
35. M.J. Rice and Y.R. Wang, preprint.

DL/1113/87/2

TECHNICAL REPORT DISTRIBUTION LIST, GEN

	No. Copies
Office of Naval Research Attn: Code 1113 800 N. Quincy Street Arlington, Virginia 22217-5000	2
Dr. Bernard Douda Naval Weapons Support Center Code 50C Crane, Indiana 47522-5050	1
Naval Civil Engineering Laboratory Attn: Dr. R. W. Drisko, Code L52 Port Hueneme, California 93401	1
Defense Technical Information Center Building 5, Cameron Station Alexandria, Virginia 22314	12 high quality
DTNSRDC Attn: Dr. H. Singerman Applied Chemistry Division Annapolis, Maryland 21401	1
Dr. William Tolles Superintendent Chemistry Division, Code 6100 Naval Research Laboratory Washington, D.C. 20375-5000	1
Dr. David Young Code 334 NORDA NSTL, Mississippi 39529	1
Naval Weapons Center Attn: Dr. Ron Atkins Chemistry Division China Lake, California 93555	1
Scientific Advisor Commandant of the Marine Corps Code RD-1 Washington, D.C. 20380	1
U.S. Army Research Office Attn: CRD-AA-IP P.O. Box 12211 Research Triangle Park, NC 27709	1
Mr. John Boyle Materials Branch Naval Ship Engineering Center Philadelphia, Pennsylvania 19112	1
Naval Ocean Systems Center Attn: Dr. S. Yamamoto Marine Sciences Division San Diego, California 91232	1

ABSTRACTS DISTRIBUTION LIST, 056/625/629

Dr. F. Carter
Code 6170
Naval Research Laboratory
Washington, D.C. 20375-5000

Dr. Richard Colton
Code 6170
Naval Research Laboratory
Washington, D.C. 20375-5000

Dr. Dan Pierce
National Bureau of Standards
Optical Physics Division
Washington, D.C. 20234

Dr. R. G. Wallis
Department of Physics
University of California
Irvine, California 92664

Dr. D. Ramaker
Chemistry Department
George Washington University
Washington, D.C. 20052

Dr. J. C. Hemminger
Chemistry Department
University of California
Irvine, California 92717

Dr. T. F. George
Chemistry Department
University of Rochester
Rochester, New York 14627

Dr. G. Rubloff
IBM
Thomas J. Watson Research Center
P.O. Box 218
Yorktown Heights, New York 10598

Dr. J. Baldeschwieler
Department of Chemistry and
Chemical Engineering
California Institute of Technology
Pasadena, California 91125

Dr. Galen D. Stucky
Chemistry Department
University of California
Santa Barbara, CA 93106

Dr. A. Steckl
Department of Electrical and
Systems Engineering
Rensselaer Polytechnic Institute
Troy, New York 12181

Dr. John T. Yates
Department of Chemistry
University of Pittsburgh
Pittsburgh, Pennsylvania 15260

Dr. R. Stanley Williams
Department of Chemistry
University of California
Los Angeles, California 90024

Dr. R. P. Messmer
Materials Characterization Lab.
General Electric Company
Schenectady, New York 22217

Dr. J. T. Keiser
Department of Chemistry
University of Richmond
Richmond, Virginia 23173

Dr. R. W. Plummer
Department of Physics
University of Pennsylvania
Philadelphia, Pennsylvania 19104

Dr. E. Yeager
Department of Chemistry
Case Western Reserve University
Cleveland, Ohio 41106

Dr. N. Winograd
Department of Chemistry
Pennsylvania State University
University Park, Pennsylvania 16802

Dr. Roald Hoffmann
Department of Chemistry
Cornell University
Ithaca, New York 14853

Dr. Robert L. Whetten
Department of Chemistry
University of California
Los Angeles, CA 90024

Dr. Daniel M. Neumark
Department of Chemistry
University of California
Berkeley, CA 94720

Dr. G. M. Morrison
Department of Chemistry
Cornell University
Ithaca, New York 14853

ABSTRACTS DISTRIBUTION LIST, 056/625/629

Dr. J. E. Jensen
Hughes Research Laboratory
3011 Malibu Canyon Road
Malibu, California 90265

Dr. J. H. Weaver
Department of Chemical Engineering
and Materials Science
University of Minnesota
Minneapolis, Minnesota 55455

Dr. A. Reisman
Microelectronics Center of North Carolina
Research Triangle Park, North Carolina
27709

Dr. M. Grunze
Laboratory for Surface Science
and Technology
University of Maine
Orono, Maine 04469

Dr. J. Butler
Naval Research Laboratory
Code 6115
Washington D.C. 20375-5000

Dr. L. Interante
Chemistry Department
Rensselaer Polytechnic Institute
Troy, New York 12181

Dr. Irvin Heard
Chemistry and Physics Department
Lincoln University
Lincoln University, Pennsylvania 19352

Dr. K. J. Klaubunde
Department of Chemistry
Kansas State University
Manhattan, Kansas 66506

Dr. C. B. Harris
Department of Chemistry
University of California
Berkeley, California 94720

Dr. R. Bruce King
Department of Chemistry
University of Georgia
Athens, Georgia 30602

Dr. R. Reeves
Chemistry Department
Renssaeler Polytechnic Institute
Troy, New York 12181

Dr. Steven M. George
Stanford University
Department of Chemistry
Stanford, CA 94305

Dr. Mark Johnson
Yale University
Department of Chemistry
New Haven, CT 06511-8118

Dr. W. Knauer
Hughes Research Laboratory
3011 Malibu Canyon Road
Malibu, California 90265

Dr. Theodore E. Madey
Surface Chemistry Section
Department of Commerce
National Bureau of Standards
Washington, D.C. 20234

Dr. J. E. Demuth
IBM Corporation
Thomas J. Watson Research Center
P.O. Box 218
Yorktown Heights, New York 10598

Dr. M. G. Lagally
Department of Metallurgical
and Mining Engineering
University of Wisconsin
Madison, Wisconsin 53706

Dr. R. P. Van Duyne
Chemistry Department
Northwestern University
Evanston, Illinois 60637

Dr. J. M. White
Department of Chemistry
University of Texas
Austin, Texas 78712

Dr. Richard J. Saykally
Department of Chemistry
University of California
Berkeley, California 94720

ABSTRACTS DISTRIBUTION LIST, 056/625/629

Dr. G. A. Somorjai
Department of Chemistry
University of California
Berkeley, California 94720

Dr. J. Murday
Naval Research Laboratory
Code 6170
Washington, D.C. 20375-5000

Dr. W. T. Peria
Electrical Engineering Department
University of Minnesota
Minneapolis, Minnesota 55455

Dr. Keith H. Johnson
Department of Metallurgy and
Materials Science
Massachusetts Institute of Technology
Cambridge, Massachusetts 02139

Dr. S. Sibener
Department of Chemistry
James Franck Institute
5640 Ellis Avenue
Chicago, Illinois 60637

Dr. Arold Green
Quantum Surface Dynamics Branch
Code 3817
Naval Weapons Center
China Lake, California 93555

Dr. A. Wold
Department of Chemistry
Brown University
Providence, Rhode Island 02912

Dr. S. L. Bernasek
Department of Chemistry
Princeton University
Princeton, New Jersey 08544

Dr. W. Kohn
Department of Physics
University of California, San Diego
La Jolla, California 92037

Dr. Stephen D. Kevan
Physics Department
University Of Oregan
Eugene, Oregon 97403

Dr. David M. Walba
Department of Chemistry
University of Colorado
Boulder, CO 80309-0215

Dr. L. Kesmodel
Department of Physics
Indiana University
Bloomington, Indiana 47403

Dr. K. C. Janda
University of Pittsburg
Chemistry Building
Pittsburg, PA 15260

Dr. E. A. Irene
Department of Chemistry
University of North Carolina
Chapel Hill, North Carolina 27514

Dr. Adam Heller
Bell Laboratories
Murray Hill, New Jersey 07974

Dr. Martin Fleischmann
Department of Chemistry
University of Southampton
Southampton SO9 5NH
UNITED KINGDOM

Dr. H. Tachikawa
Chemistry Department
Jackson State University
Jackson, Mississippi 39217

Dr. John W. Wilkins
Cornell University
Laboratory of Atomic and
Solid State Physics
Ithaca, New York 14853

Dr. Ronald Lee
R301
Naval Surface Weapons Center
White Oak
Silver Spring, Maryland 20910

Dr. Robert Gomer
Department of Chemistry
James Franck Institute
5640 Ellis Avenue
Chicago, Illinois 60637

Dr. Horia Metiu
Chemistry Department
University of California
Santa Barbara, California 93106

Dr. W. Goddard
Department of Chemistry and Chemical
Engineering
California Institute of Technology
Pasadena, California 91125